Finite element implementation of anisotropic quasilinear viscoelasticity using a discrete spectrum approximation

Michael A. Puso
Methods Development Group, Lawrence Livermore National Laboratory
Livermore, California 94550

and

Jeffrey A. Weiss
Orthopedic Biomechanics Institute
Department of Bioengineering, University of Utah
Salt Lake City, Utah 84107
and
Applied Mechanics Group, Lawrence Livermore National Laboratory
Livermore, California 94550

In Press, *ASME Journal of Biomechanical Engineering*
January 16, 1997

Corresponding Author:
Jeffrey A. Weiss
Orthopedic Biomechanics Institute
5848 South 300 East
Salt Lake City, Utah 84107
801-269-4035
jeff@osiris.usi.utah.edu

Keywords: quasilinear viscoelasticity, finite element, soft tissue mechanics, constitutive modeling

Abstract

The objective of this work was to develop a theoretical and computational framework to apply the finite element method to anisotropic, viscoelastic soft tissues. The quasilinear viscoelastic (QLV) theory provided the basis for the development. To allow efficient and easy computational implementation, a discrete spectrum approximation was developed for the QLV relaxation function. This approximation provided a graphical means to fit experimental data with an exponential series. A transversely isotropic hyperelastic material model developed for ligaments and tendons was used for the elastic response. The viscoelastic material model was implemented in a general-purpose, nonlinear finite element program. Test problems were analyzed to assess the performance of the discrete spectrum approximation and the accuracy of the finite element implementation. Results indicated that the formulation can reproduce the anisotropy and time-dependent material behavior observed in soft tissues. Application of the formulation to the analysis of the human femur-medial collateral ligament-tibia complex demonstrated the ability of the formulation to analyze large three-dimensional problems in the mechanics of biological joints.

Introduction

Recent advances in computational mechanics and computer hardware have provided the biomechanics community with the tools to develop large-scale finite element models of biological joints. Models of this nature offer the ability to predict soft tissue stresses, joint contact forces, and joint kinematics for externally applied loads and displacements. Three-dimensional constitutive laws for the soft tissues are necessary for the development of these models. In particular, because ligaments and tendons have inherently three-dimensional geometry and can transfer forces to other soft and hard tissues, they require an explicit three-dimensional representation.

The time- and rate-dependent material behavior of soft tissues has been well-documented and quantified in the literature over the past 20 years. This has included ligaments [Woo et al., 1981], tendons [Johnson et al., 1994, Pradas and Calleja, 1990], articular cartilage [Setton et al., 1993, Woo et al., 1980], heart and skeletal muscle [Best et al., 1994, Pinto and Patitucci, 1980] and cell membranes [Duszyk et al., 1989]. This behavior can arise from fluid flow in or out of the tissue, from inherent viscoelasticity of the solid phase, or from viscous interactions

between tissue components or phases [Mak, 1986]. A theory of quasilinear viscoelasticity (QLV) has been proposed by Fung and is widely used in the field of biomechanics to describe soft tissue viscoelastic behavior [Fung, 1981]. The basis of the theory is that 1) the stress at a given time can be described by a convolution integral representation, separating the elastic response and the relaxation function, and 2) that the relaxation function has a continuous spectrum. This representation has successfully described and predicted experimental data. For instance, using the QLV theory, Johnson et al. [Johnson et al., 1994] showed that the viscoelastic properties of human patellar tendon from both young and old donors could be described. Studies such as these have restricted the experimental testing to achieve one-dimensional test situations.

To use the QLV theory for the description or prediction of soft tissue material response in three dimensions, an appropriate three-dimensional elastic response function must be selected. Often the framework of hyperelasticity has been used to dictate the choice of this tensor function based on considerations of material symmetry [Fung, 1981, Guccione et al., 1991, Humphrey and Yin, 1987, Spencer, 1984, Weiss et al., 1995a, Weiss, 1995]. Because biological soft tissues often contain of one or more families of reinforcing fibers (collagen or elastin), the tissues exhibit an anisotropic elastic response. Humphrey used this approach, selecting a transversely isotropic elastic strain energy to describe and predict the material response of cardiac muscle [Humphrey and Yin, 1987]. There have been numerous elastic constitutive laws proposed for representing the quasistatic behavior of soft tissues, however only a handful have allowed for three-dimensional, anisotropic material behavior (i.e., [Guccione et al., 1991, Horowitz et al., 1988, Humphrey et al., 1990, Lanir, 1983, Weiss, 1995]. Researchers have yet to develop a finite element implementation that allows the analysis of viscoelastic soft tissues with an anisotropic elastic response. This is necessary to accurately simulate the material behavior of soft tissues in a finite element context.

A number of basic and applied research questions can be answered using a computational simulation of soft tissue viscoelastic material behavior. For instance, tissue viscoelasticity plays a critical role in the response of biological joints to high-rate loading or impact scenarios. The stiffening effect of the viscoelastic phase and large pointwise variations in strain rate can greatly influence soft tissue stresses. Also, there has been recent experimental work that has shown the importance of solid-phase viscoelasticity in the mechanics of biphasic materials [Setton et al., 1993]. The integration of solid phase viscoelasticity into biphasic constitutive

models follows directly by substituting the appropriate time-varying stress representation for the solid material properties, as is done in standard solid viscoelasticity [Mak, 1986]. This approach can provide new insight into the structural significance of the solid phase in bearing transient loads to the soft tissues. Closed-form solutions to these and many other problems of interest are intractable because of complex geometry and boundary/initial conditions, geometric and material nonlinearities. The finite element method addresses these issues.

Despite the importance of viscoelastic soft tissue behavior in biomechanics research, a finite element implementation for the QLV theory is not available. The most troublesome difficulty in constructing such an implementation is that information must be saved at every computational timestep in order to compute the stress response at the current timestep. The computer storage requirements for this type of approach are prohibitive. This is a direct result of the continuous relaxation spectrum used in the convolution representation for the QLV theory. Additionally, there have been few finite element implementations of an anisotropic hyperelastic constitutive models [Guccione et al., 1991, Horowitz et al., 1988, Weiss et al., 1995a].

To allow for the large-scale simulation of anisotropic viscoelastic soft tissue behavior, an accurate and efficient finite element implementation is necessary. The objective of this work was to develop a theoretical and computational framework for modeling viscoelastic soft tissues that accommodated anisotropic material symmetry. This was pursued using the finite element method, a discrete spectrum approximation to the theory of quasilinear viscoelasticity, and a transversely isotropic elastic response function.

Methods

The methods are divided into four distinct sections - "Theoretical Background, "Discrete Spectrum Approximation", "Transversely Isotropic Elastic Response", and "Finite Element Implementation". The latter three represent original theoretical and methodological results. The final section of the Methods, "Test Problems", describes analyses that were conducted to assess the performance of the discrete spectrum approximation and the accuracy and efficiency of the finite element formulation.

Theoretical Background

Following standard notational conventions [Spencer, 1984], $\mathbf{X}$ is chosen to represent the position of a particle in the reference configuration, while $\mathbf{x}$ represents the particle in the deformed (current) configuration. The *deformation gradient*, $\mathbf{F}$, is defined as

$$\mathbf{F}(\mathbf{X}) \;:=\; \partial \mathbf{x}/\partial \mathbf{X}. \tag{1}$$

The *right Cauchy-Green deformation* tensor is then

$$\mathbf{C} \;:=\; \mathbf{F}^T\mathbf{F}. \tag{2}$$

The QLV theory assumes that the 2nd Piola-Kirchhoff stress $\mathbf{S}(t)$ can be written as the convolution of a relaxation function $G(t)$ with an elastic response function $\mathbf{S}^e$ (Note that in general, the scalar-valued relaxation function could be replaced by a 4th-order tensor to produce direction-dependent relaxation phenomena). The elastic response $\mathbf{S}^e$ will be chosen to correspond to a transversely isotropic hyperelastic constitutive model recently proposed for fiber-reinforced soft tissues, to be discussed shortly [Weiss, 1994, Weiss, 1995]. If the motion starts at $t = 0$ and the stress and strain are zero prior to this time,

$$\mathbf{S}(t) \;=\; \int_0^t G\left(t-s\right) \frac{\mathrm{d}\mathbf{S}^e}{\mathrm{d}s} \mathrm{d}s. \tag{3}$$

Fung proposed a continuous relaxation function adapted from [Neubert, 1963] to describe the behavior of biological soft tissues:

$$G(t) \;=\; \frac{\left\{1 + c\left[E_1\left(t/\tau_2\right) - E_1\left(t/\tau_1\right)\right]\right\}}{1 + c\ln\left(\tau_2/\tau_1\right)}, \tag{4}$$

where $E_1(t)$ is the exponential integral function,

$$E_1(t) \;=\; \int_z^\infty \frac{\mathrm{e}^{-t}}{t} \mathrm{d}t. \tag{5}$$

The stiffness (real part of the complex modulus) for the QLV relaxation kernel given by (4) is [Fung, 1981]

$$\text{stiffness} \;=\; \frac{\ln\left[\left(\omega\tau_2\right)^2 + 1\right] - \ln\left[\left(\omega\tau_1\right)^2 + 1\right]}{2\ln\left(\frac{\tau_2}{\tau_1}\right)}, \tag{6}$$

while the damping (imaginary part of the complex modulus) is given by

$$\text{damping} \;=\; \frac{\tan^{-1}\left(\omega\tau_2\right) - \tan^{-1}\left(\omega\tau_1\right)}{\ln\left(\frac{\tau_2}{\tau_1}\right)}. \tag{7}$$

Both the stiffness and damping are unitless.

The relaxation function (4) has a smooth, linear decrease from short to long relaxation times (Figure 1A). The stiffness (6) increases with increasing frequency, while the damping (7) is relatively constant over a wide range of frequencies [Tschoegl, 1989] (Figure 1B). This yields a hysteresis loop that is relatively insensitive to strain rate over several decades, a feature often observed for soft tissues. The three viscoelastic material coefficients, τ_1, τ_2, and c, are determined from appropriate experiments.

In an implicitly integrated finite element code using an incremental solution strategy, the solution is known at time t, and the task is to determine the solution at $t + \Delta t$ using an iterative (Newton) method [Bathe, 1982]. The stress at time $t + \Delta t$ can be written as the sum of two integrals:

$$\mathbf{S}(t+\Delta t) = \int_0^t G(t+\Delta t-s)\frac{\mathrm{d}\mathbf{S}^e}{\mathrm{d}s}\mathrm{d}s + \int_t^{t+\Delta t} G(t+\Delta t-s)\frac{\mathrm{d}\mathbf{S}^e}{\mathrm{d}s}\mathrm{d}s. \tag{8}$$

The second term in (8) can be rewritten using the Mean Value Theorem:

$$\int_t^{t+\Delta t} G(t+\Delta t-s)\frac{\mathrm{d}\mathbf{S}^e}{\mathrm{d}s}\mathrm{d}s = \frac{\mathrm{d}\mathbf{S}^e(\xi)}{\mathrm{d}s}\int_t^{t+\Delta t} G(t+\Delta t-s)\,\mathrm{d}s, \tag{9}$$

where $\xi \in [t, t+\Delta t]$. Approximating $\mathrm{d}\mathbf{S}^e/\mathrm{d}s$ with a central difference rule,

$$\int_t^{t+\Delta t} G(t+\Delta t-s)\frac{\mathrm{d}\mathbf{S}^e}{\mathrm{d}s}\mathrm{d}s \cong \int_t^{t+\Delta t} G(t+\Delta t-s)\,\mathrm{d}s\left[\frac{\mathbf{S}^e_{t+\Delta t}-\mathbf{S}^e_t}{\Delta t}\right]. \tag{10}$$

The right-hand side of (10) can be evaluated exactly at time $t + \Delta t$ provided that the stress $\mathbf{S}^e$ is available from the last timestep. The central difference approximation is second-order accurate. However, the evaluation of the first integral in (8) requires $\mathbf{S}^e$ from all previous times. This requires storage for a symmetric 2nd order tensor at each integration point, for each element, at each previous timestep. For even the smallest problems, these storage requirements are prohibitive. Additionally, a uniform approach to integrate the first integral over time is not available. The accuracy of any such integration scheme would be highly dependent on the timestep size. These problems are addressed below.

Discrete Spectrum Approximation

If the reduced relaxation function $G(t-s)$ is an exponential, a recurrence relation can be exploited to evaluate the first integral in (8). Specifically, consider the case when

$$G(t) = C_1 \exp(-t/\nu). \tag{11}$$

The first integral in (8) becomes

$$\begin{aligned} & \int_0^t C_1 \exp\left(-\left(t+\Delta t-s\right)/\nu\right) \frac{\mathrm{d}\mathbf{S}^e}{\mathrm{d}s}\mathrm{d}s \qquad (12) \\ = \;& \exp\left(-\Delta t/\nu\right) \int_0^t C_1 \exp\left(-\left(t-s\right)/\nu\right) \frac{\mathrm{d}\mathbf{S}^e}{\mathrm{d}s}\mathrm{d}s \\ = \;& \exp\left(-\Delta t/\nu\right) \mathbf{S}\left(t\right). \end{aligned}$$

Note that only the stress $\mathbf{S}\left(t\right)$ from the last timestep is needed to evaluate the integral.

To use this framework for Fung's reduced relaxation function, an exponential series approximation to (4) was developed. A log plot of (4) shows a linear transition region between short and long times (Figure 1A). A series of exponentials with equal spectral strengths and relaxation times spread one decade apart provides such qualitative behavior [Tschoegl, 1989]. Based on this observation, the following approximation to (4) was made:

$$G\left(t\right) \;=\; G_e + \frac{G_0 - G_e}{N_d + 1} \sum_{I=0}^{N_d} \exp\left(t/10^{(I+I_0)}\right), \qquad (13)$$

where G_e is the equilibrium modulus, G_0 is the initial modulus, N_d is the span of the transition region in decades, and 10^{I_0} is the lowest discernible relaxation time. The span of the transition region is chosen so that it includes the nonlinear curve sections on each end of the central, linear region, as shown in Figure 1A. This ensures that the transition regions will be represented accurately in the discrete spectrum approximation. All required coefficients G_e, G_0, N_d and I_0 can be determined graphically from a log plot of $G\left(t\right)$, as in Figure 1A.

With (13) chosen for the relaxation function, the viscoelastic 2nd Piola-Kirchoff stress at time $t+\Delta t$ can be written as:

$$\mathbf{S}\left(t+\Delta t\right) = \int_0^{t+\Delta t} \left(G_e + K \sum_{I=0}^{N_d} \exp(t+\Delta t - s/\nu_I) \right) \frac{\mathrm{d}\mathbf{S}^e\left(s\right)}{\mathrm{d}s}\mathrm{d}s \qquad (14)$$

$$\begin{aligned} = \;& G_e \mathbf{S}^e\left(t+\Delta t\right) \\ + \;& K \sum_{I=0}^{N} \left[\exp\left(-\Delta t/\nu_I\right) \mathbf{H}_I\left(t\right) + \left(\mathbf{S}^e\left(t+\Delta t\right) - \mathbf{S}^e\left(t\right)\right) \frac{\left(1-\exp\left(-\Delta t/\nu_I\right)\right)}{\Delta t/\nu_I} \right], \qquad (15) \end{aligned}$$

where

$$K \;:=\; \frac{G_0 - G_e}{N_d + 1} \;\text{ and }\; \nu_I \;:=\; 10^{I+I_0}, \qquad (16)$$

and the history variables $\mathbf{H}_I$ (each a symmetric 2nd order tensor) are defined as:

$$\mathbf{H}_I \;:=\; \int_0^t \exp\left(-\left(t-s\right)/\nu_I\right) \frac{\mathrm{d}\mathbf{S}^e\left(s\right)}{\mathrm{d}s}\mathrm{d}s. \qquad (17)$$

Now the tensor quantities $\mathbf{S}^e(t)$ and $\mathbf{S}^e(t+\Delta t)$ can be computed at time $t+\Delta t$, as can all other scalar quantities. Only the $\mathbf{H}_I$ must be stored from the last timestep.

In addition to the stress $\mathbf{S}^e(t+\Delta t)$, the fourth order elasticity tensor $\mathsf{C}(t+\Delta t)$ is needed to form the stiffness matrix for the finite element solution procedure [Bathe, 1982]. C is defined as:

$$\mathsf{C}(t+\Delta t) := 2\frac{\partial \mathbf{S}(t+\Delta t)}{\partial \mathbf{C}(t+\Delta t)}, \tag{18}$$

where $\mathbf{C}(t+\Delta t)$ is the right Cauchy-Green deformation tensor at time $(t+\Delta t)$. Using the above definition with (15) and noting that only $\mathbf{S}^e(t+\Delta t)$ depends on $\mathbf{C}(t+\Delta t)$,

$$\mathsf{C}(t+\Delta t) = \left[G_e + K\sum_{I=0}^{N}\frac{(1-\exp(-\Delta t/\nu_I))}{\Delta t/\nu_I}\right] 2\frac{\partial \mathbf{S}^e(t+\Delta t)}{\partial \mathbf{C}(t+\Delta t)}. \tag{19}$$

$$= \left[G_e + K\sum_{I=0}^{N}\frac{(1-\exp(-\Delta t/\nu_I))}{\Delta t/\nu_I}\right] \mathsf{C}^0(t+\Delta t). \tag{20}$$

Here, $\mathsf{C}^0(t+\Delta t)$ is the "time-zero" elasticity tensor. Thus the modification of the stiffness to extend the elastic case to viscoelasticity involves only multiplying the components of C^0 by a scalar quantity.

Transversely Isotropic Elastic Response

The discrete spectrum approximation for the QLV kernel and the approach for its finite element implementation can accommodate *any* elastic response. A particular elastic response was chosen for implementation to represent incompressible, transversely isotropic soft tissues, and is described below. Further details of the development and implementation of this constitutive model can be found in [Weiss, 1994, Weiss et al., 1995a, Weiss, 1995].

A unit vector field $\mathbf{a}^0$ in the undeformed configuration is used to describe the local fiber direction, and the strain energy is required to depend on this vector. By standard arguments [Marsden and Hughes, 1983], the strain energy is then an isotropic function of $\mathbf{C}$ and $\mathbf{a}^0$. When the material undergoes deformation, $\mathbf{a}^0(\mathbf{X})$ will deform with the body. After deformation, the fiber direction may be described by a unit vector field $\mathbf{a}(\mathbf{x}(\mathbf{X}))$. In general the fibers will also undergo length change. The fiber stretch, λ, is then

$$\lambda\mathbf{a} = \mathbf{F}\cdot\mathbf{a}^0, \tag{21}$$

where $\mathbf{F}$ is the deformation gradient tensor. A material with the above symmetry is *transversely isotropic.*

The elastic response of the tissue was assumed to arise from the resistance of the collagen fiber family, the ground substance matrix, and their interaction. Further, it was assumed that the ground substance, or matrix, was isotropic. Finally, the composite structure was assumed incompressible because of the large amount of trapped water in the tissue. With these assumptions, the strain energy can be written as:

$$W = F_1(I_1, I_2) + F_2(\lambda) + F_3(I_1, I_2, \lambda) \tag{22}$$

The function F_1 represents the material response of the isotropic ground substance matrix, F_2 represents the contribution from the collagen fiber family, and F_3 is the contribution from interactions between the fibers and matrix, such as a shear coupling. I_1 and I_2 are the standard invariants of the right Cauchy-Green deformation tensor and are the complete set of invariants associated with incompressible isotropic material behavior:

$$I_1 = \mathrm{tr}\mathbf{C}, \qquad I_2 = \frac{1}{2}\left[(\mathrm{tr}\mathbf{C})^2 - \mathrm{tr}\mathbf{C}^2\right]. \tag{23}$$

The dependence on λ arises directly from the reinforcing fiber family.

For a hyperelastic material, the 2nd Piola-Kirchhoff stress is derived from W. The stress for an incompressible hyperelastic material with strain energy given by (22) is

$$\mathbf{S}^e = 2\frac{\partial W}{\partial \mathbf{C}} = 2\left\{(W_1 + I_1 W_2)\,\mathbf{1} - W_2\mathbf{C}\right\} + \frac{1}{\lambda}W_\lambda \mathbf{a}^0 \otimes \mathbf{a}^0 + p\mathbf{C}^{-1}. \tag{24}$$

For (22), the following identifications can be made in (24):

$$W_1 = \frac{\partial F_1}{\partial I_1} + \frac{\partial F_3}{\partial I_1}, \quad W_2 = \frac{\partial F_1}{\partial I_2} + \frac{\partial F_3}{\partial I_2}, \quad W_\lambda = \frac{\partial F_2}{\partial \lambda} + \frac{\partial F_3}{\partial \lambda}. \tag{25}$$

Equation (22) generalizes many constitutive equations that have been successfully used in the past to describe biological soft tissues such as cardiac muscle [Choung and Fung, 1986, Horowitz et al., 1988, Humphrey et al., 1990, Humphrey and Yin, 1987].

A simplified form of the function (22) was chosen for the elastic response in the QLV implementation. The intent was to demonstrate the characteristics of the strain energy function without including the interaction term F_3, for which experimental data are not currently available. The Mooney-Rivlin model [Mooney, 1940] was used for the matrix:

$$F_1 = \frac{C_1}{2}(I_1 - 3) + \frac{C_2}{2}(I_2 - 3). \tag{26}$$

Several observations about the mechanical behavior of collagen fibers were incorporated into the form for F_2. First, collagen does not support a significant compressive load, and

structures that are composed of mostly collagen will tend to buckle under very small compressive forces. Second, the tensile stress-stretch relation for ligaments and tendons can be well-approximated by an exponential in the toe region and subsequently by a line. These observations led to the following choice for the strain energy derivatives of the collagen fibers:

$$\begin{aligned} W_\lambda &= 0, && \lambda \leq 1, \\ W_\lambda &= C_3 \left(\exp \left(\mathrm{C}_4 \left(\lambda - 1 \right) \right) - 1 \right), && 1 < \lambda < \lambda^*, \\ W_\lambda &= C_5 \lambda + C_6, && \lambda \geq \lambda^*. \end{aligned} \tag{27}$$

Here, λ^* is the stretch at which the collagen fibers are straightened, C_3 scales the exponential stresses, C_4 is the rate of collagen fiber uncrimping, and C_5 is the modulus of the straightened collagen. The y-intercept of the linear region, C_6, was determined from the condition that the stress is C^0 continuous at λ^*:

$$C_6 = C_3 \left(\exp \left(\mathrm{C}_4 \left(\lambda^* - 1 \right) \right) - 1 \right) - C_5 \lambda^* \tag{28}$$

This transversely isotropic elastic response function has been successfully used to describe and predict the quasistatic response of human fascia lata, both along and transverse to the collagen fiber direction [Weiss, 1994, Weiss, 1995].

Finite Element Implementation

The finite element implementation of the transversely isotropic constitutive model described above was extended to quasilinear viscoelasticity to allow computational simulation of anisotropic viscoelastic material behavior. This was performed using the general-purpose nonlinear finite element code, NIKE3D, developed and maintained at Lawrence Livermore National Laboratory [Maker et al., 1990]. For speed of computation, the formulation was based on the three-dimensional eight-node hexahedral element. Following Simo and Taylor, separate interpolation for the displacement, pressure and dilation were used on the element level to avoid "locking" for nearly and fully incompressible material behavior [Simo et al., 1985]. Eight-point Gaussian quadrature was used to evaluate integrals involving the incremental displacements and element geometry, while integral involving the pressure and dilation were evaluated at the element center. Since the integrals involving pressure and dilation could be expressed in terms of the incremental displacements on an element, these variables were eliminated at the element level, yielding a "generalized displacement" approach [Weiss et al., 1995a]. For

the case of fully incompressible behavior, the method of augmented Lagrangians was used to enforce the constraint to a user-specified accuracy [Simo and Taylor, 1991].

For the fiber direction vector field $\mathbf{a}^0$ in the elastic response (Equation 24), the local collagen direction was defined either based on global vector or local element geometry. In the latter method, the local collagen fiber direction at each element integration point was based on the edge orientation of the element. The local element "i", "j" or "k" direction was chosen based on a flag in the input deck. The element edge direction defining curves from the tibial to femoral insertions was chosen as the fiber direction for the analyses.

Test Problems

To assess the performance of the discrete spectrum approximation and the accuracy and efficiency of the finite element formulation, a series of numerical tests were carried out. Except where indicated, the coefficients for the QLV relaxation function were taken from [Woo et al., 1981] (Table 1B), while the coefficients for the transversely isotropic elastic response were taken from [Weiss, 1994, Weiss, 1995] (Table 1A). All computations were carried out on a Silicon Graphics Power Indigo2 workstation.

One-Element Test. To verify the implementation, illustrate the characteristics of the anisotropic elastic response, and show the viscoelastic behavior, the response of a single element to equibiaxial stretch followed by stress relaxation was examined. Because the equibiaxial stretch state represented a homogeneous deformation, only a single element was needed to reproduce the deformation state exactly. The stretch directions were chosen to be along and transverse to the collagen fiber direction. The following material coefficients were used to illustrate the large-deformation behavior of the model and its salient features: $C_1 = 10.0$ KPa, $C_2 = 10.0$ KPa, $C_3 = 0.7$ KPa, $C_4 = 10.0$, $C_5 = 1100.0$ KPa, $\lambda^* = 1.6$. The discrete series approximation of the coefficients in Table 1B were used for the viscoelastic response (Table 1C). The single element was elongated from 0 to 100% from $t = 0$ seconds to $t = 1$ seconds. The elongation was held constant and the stress relaxed until $t = 3$ seconds.

Modeling of Ligament Cyclic Stress Relaxation. To simulate the cyclic subfailure tensile test that is used by soft tissue researchers to precondition samples before failure testing, a block of 125 elements (5x5x5) was assigned the material properties in Table 1 and subjected to cyclic loading via applied displacement boundary conditions. The mesh was stretched from 0 to 3% strain over a 5 second time interval, followed by cyclic stretching from

1.5 - 3.0% strain at a rate of 0.1 Hz. The timestepping algorithm was adjusted to ensure that a solution was obtained at each peak and valley in the applied strain profile.

Finite Element Model of Human Medial Collateral Ligament (MCL). To illustrate the performance of the visco-hyperelastic material model in a large-scale finite element problem, a model of the human femur-MCL-tibia complex was constructed for simulation of valgus rotational loading. Polygonal surfaces of the distal femur, proximal tibia and superficial MCL were obtained from a commercial supplier (Viewpoint Datalabs, Orem, UT). The polygon data were imported into a commercial block-structured mesh generator (XYZ Scientific Applications, Livermore, CA). Hexahedral block-structured meshes of the three structures were constructed by projecting the element faces onto the polygonal surfaces. The final computational mesh consisted of 6,000, 1,296 and 400 8-noded hexahedral elements for the femur, tibia and MCL, respectively.

To illustrate the rate-dependence of the soft tissue stresses, analyses were carried out using both the hyperelastic and visco-hyperelastic materials. For the hyperelastic material case, coefficients in Table 1A were used. For the viscoelastic material case, coefficients in Tables 1A and 1C were used. To decrease the computational expense, the bones were represented using a rigid material model [Maker, 1994], reducing the number of degrees of freedom to six for each rigid body. These degrees of freedom consisted of three translations and three rotations with respect to coordinate systems embedded within the bones.

The motion of each bone was controlled by the six degrees of freedom for each bone via load curves, specifying their value as a function of time. An incremental-iterative solution strategy was used [Bathe, 1982]. Using the knee joint coordinate system described by Grood and Suntay [Grood and Suntay, 1983], the tibia was held fixed while all but the varus-valgus rotation were fixed for the femur. To allow attachment of the MCL ends to the bones without conformity of the finite element mesh, the last row of elements on each end of the MCL was specified to be the same (rigid) material as the bone to which it attached.

Frictionless sliding interfaces were used to model the MCL-femur and MCL-tibia contact [Hallquist et al., 1985]. The contact constraint was enforced using a standard penalty implementation. Contact surface penalties were chosen so that the maximum penetration distance would not exceed 0.2 mm at any point on the contact surfaces during the analysis.

The MCL was first tensioned to a level of 3% strain using a previously described methodology [Weiss et al., 1995b]. The procedure allows the specification of the initial stretch along

the fiber direction (λ) as a function of time for each element in the mesh. The initial stretch data was specified via a load curve. For the viscoelastic material case, the stress in the MCL was then allowed to relax. For both material cases, the knee was subjected to a valgus rotation of 5 degrees. This value was chosen based on in vivo studies that have shown the human knee can tolerate 5 degrees valgus rotation without failure while tibial axial rotation is constrained [Mills and Hull, 1991]. The valgus rotation was applied at a rate of 50 degrees/second. Automatic timestepping strategy and a quasi-Newton nonlinear solver were used [Bathe, 1982, Maker et al., 1990]. The linear system consisted of 126,259 degrees of freedom, but was reduced to 2,377 after the condensation procedure for the rigid elements.

Results

Discrete Spectrum Approximation

Comparing the relaxation function $G(t)$ computed from the continuous spectrum (4) and the discrete series approximation (13), excellent agreement was obtained using parameters determined graphically from the time plot of (4) (Figure 1A, $R^2 = 0.986$). The real and imaginary parts of the complex modulus for both the continuous and discrete spectra were computed and plotted as a function of frequency (Figure 1B). Again, good agreement was achieved. This illustrates that the simple graphical method of determining the coefficients for the discrete relaxation spectrum provides a quick and accurate means of fitting the continuous spectrum with an exponential series.

Finite Element Implementation

Because up to six relaxation terms were used in the finite element implementation, additional storage was required for the stress contribution from each term, requiring (6 terms) x (6 stress components) x (8 integration points) = 288 additional words of storage for each element *for only the last timestep*. The use of the recurrence relation bypassed the need to allocate this much storage for every past timestep. Additionally, the integration of the viscoelastic stress terms in equation (8) were easily implemented using the recurrence relationship illustrate for the one-exponential relaxation function by equation (13). The elasticity tensor needed to form the stiffness matrix was formed directly from the existing time-zero elasticity tensor, as shown in equation (20). Because implementation of the elasticity tensor is often the most

difficult part of adding new material models, this fact offered a significant savings in effort from a programming standpoint.

Test Problems

One-Element Test. Several important features of the anisotropic viscoelastic model were illustrated by this test problem of equibiaxial extension (Figure 2). The stresses along the collagen fiber direction are much larger than those transverse to the fiber direction, as expected for a fiber-reinforced composite. Further, the characteristic "toe region" corresponding to uncrimping of the collagen fibrils, followed by a linear region, are easily identified in Figure 2A. In contrast, the stress-strain behavior in the transverse direction is relatively linear with increasing time up to $t = 1$. The peak viscoelastic stresses are larger than the elastic stresses. This is a direct result of the stiffening of the material with strain rate, which is predicted by the QLV model. The viscoelastic stresses begin to decay from their peak values at $t > 1$, showing the characteristic relaxation associated with viscoelastic behavior. During the entire simulation, fully incompressible material behavior was maintained using the augmented Lagrangian method.

Modeling of Ligament Cyclic Stress Relaxation. The resulting stress response were plotted as a function of time for the simulated cyclic test (Figure 3A). The peak and valley stresses were 83% and 44% of their initial values by the last cyle, and the data were very similar qualitatively to that obtained from typical preconditioning tests on ligamentous tissues. The changes in stress-strain behavior were most easily seen by examining the hysteresis curves (Figure 3B). The amount of energy lost during each cycle (area under the loading-unloading curve) decreased with increasing cycle number. The loading-unloading curves shifted downward with increasing cycle number.

Finite Element Model of Human Medial Collateral Ligament (MCL). The solution for the elastic material properties was obtained in 5.6 minutes and 13 timesteps, while the solution with viscoelastic properties took 10.8 minutes and 20 timesteps. The additional timesteps needed to obtain a solution for the viscoelastic material is a result of the increased material nonlinearity introduced by the time- and rate-dependent material properties, dictating the use of a smaller time increment with the quasi-Newton solver. The average per-step cost was 0.4 and 0.54 minutes for the elastic and viscoelastic cases, indicating a small increase in cost from the additional floating point operations of the viscoelastic model.

The magnitude of the reaction force across the MCL-femur and the MCL-tibia contact surfaces was affected by the change in material properties. The total force across the MCL-femur contact surface was 18.9 N for the elastic case and 57.2 N for the viscoelastic case. The total force across the MCL-tibia contact surface was 16.7 N for the elastic case and 41.8 N for the viscoelastic case. The difference in the reaction forces for the femoral and tibial contact surfaces are attributable to the different geometry of the bones in the contact region and the manner in which the valgus rotation was applied. The differences between the elastic and viscoelastic material cases are due to the stiffening effect in the viscoelastic material.

The effective (von Mises) stress state in the MCL was much higher when the viscoelastic material model was used (Figure 5), due to the stiffening effect at high loading rates. Average stresses in the viscoelastic model were between 20 and 30 MPa. The large stresses at the insertions were partly an artifact of the modeling strategy used to attach the ligament.

Discussion

This paper has developed the theoretical and computational methodology to study anisotropic viscoelastic soft tissue behavior using the finite element method. Additionally, this material behavior was implemented in a general-purpose finite element code and applied to several test problems. The results of these test problems demonstrated the ability to accurately and efficiently represent common soft tissue viscoelastic behavior, both in small- and large-scale computational analyses.

This is the first finite element implementation of anisotropic visco-hyperelasticity. Many other constitutive models have been proposed and used for three-dimensional anisotropic soft tissue hyperelasticity. However, only a few implementations of these constitutive models are available for finite element computations [Guccione et al., 1991, Horowitz et al., 1988, Weiss et al., 1995a]. Finite element methods for representing soft tissues as poroelastic have been available for several years (i.e., [Suh et al., 1991]). The present work fills a gap between anisotropic hyperelasticity and poroelasticity by allowing for anisotropic solid matrix viscoelasticity in a computational setting. The present implementation can accommodate any elastic response. The one presently chosen is similar in form to those developed by Humphrey and coworkers for cardiac tissue [Humphrey et al., 1990, Humphrey and Yin, 1987], in the sense that both are based on a global invariant approach to anisotropy [Spencer, 1984]. How-

ever, the presently used function incorporated the behavior attributed to the uncrimping of collagen fibers. In this sense it is similar to microstructurally based approaches proposed by Lanir and coworkers [Lanir, 1983, Lanir, 1980]. The present work provides a compromise between a completely phenomenological constitutive model and a microstructural model. The material coefficients for the collagen fibers have physical meaning, unlike a purely phenomenological approach.

There are well-known problems when using an exponential series to approximate a continuous function. The most common is that there are many combinations of exponentials that can provide an equally good fit to any particular function. Consequently, although one may identify particular exponentials with a specific relaxation mechanism within the material, the lack of uniqueness makes the interpretation of the coefficients meaningless. However, the discrete series was only used as an approximation for the actual continuous spectrum, which was fitted directly to the experimental data. This allowed the use of the recursion relation in (13). No physical meaning is attached to the coefficients G_e, G_0, N_d, and I_0.

The femur-MCL-tibia finite element model was designed to demonstrate the performance and utility of the finite element implementation for a representative problem from joint mechanics. Several assumptions made in the construction of this model could significantly affect the computed stress response. It was assumed that the initial stretch distribution in the MCL at 0 degrees knee flexion could be approximated by specifying a value of 3% strain throughout the structure. It is well-known that the strain in knee ligaments changes with joint orientation, and is never completely uniform, e.g. [Edwards et al., 1970]. Also, the model used a crude representation of ligament insertions to bone. Because there was a sudden transition from ligament material to bone in the model, the stresses near the insertions were not reliable. However, based on St. Venant's principle, the stresses away from the insertion sites should still be accurate. An ongoing experimental study by the authors is examining the initial stretch distribution in the MCL as a function of knee joint orientation, and these data will be used in future modeling of the femur-MCL-tibia complex.

Recent work has reported that ligaments undergo some volume change during tensile testing and do not behave as fully incompressible materials [Thielke et al., 1995]. This may be a result of fluid exudation from the structure under loading. If the material is represented as a poroelastic continuum composed of both solid and fluid phases, the solid component could still be incompressible. The present implementation can accommodate both compress-

ible material behavior by a simple modification of the function W to allow strain energy to be generated via volume deformation. However, experimental measurement of this dilational response is difficult and sufficient data are not presently available.

Although in the present implementation the entire 2nd Piola-Kirchhoff stress is assumed to relax viscoelastically, it is just as easy to relax the deviatoric or dilational part of the stress. Deviatoric stress relaxation is often utilized in the analysis of viscoelastic solids when the relaxation mechanism appears to be independent of pressure. The idea of separate viscoelastic behavior for the shear and bulk response for soft tissues has been touched on by [Mak, 1986]. The presently developed theoretical and computational framework can accommodate this alternative formulation with minimal modification.

Conclusions

The theoretical and computational framework for finite element implementation of incompressible, transversely isotropic visco-hyperelasticity was developed and implemented. The storage and computation requirements for the QLV model were minimized by the use of a discrete spectrum approximation for the continuous relaxation spectrum. The elastic response allowed for reinforcement from a single fiber family and was motivated based on the observed material behavior of ligaments and tendons. Test problems were presented to demonstrate the utility and accuracy of the implementation. The implementation is ideal for finite element modeling of many biological soft tissues because it accommodates both the anisotropic material properties and the viscoelasticity, the two main characteristics of these materials. The transversely isotropic visco-hyperelastic material models provide an excellent means to examine dynamic simulations of soft tissue and joint mechanics with the finite element method.

Acknowledgements

Partial support for this work was provided under the auspices of the U.S. Department of Energy by the Lawrence Livermore National Laboratory under contract # W-7405-Eng-8, and the Whitaker Foundation Biomedical Engineering Research Grants.

References

[Bathe, 1982] Bathe, K.-J. (1982). *Finite Element Procedures in Engineering Analysis.* Prentice-Hall, New Jersey.

[Best et al., 1994] Best, T., McElhaney, J., Garrett, W., and Myers, B. (1994). Characterization of the passive responses of live skeletal muscle using the quasi-linear theory of viscoelasticity. *J Biomech*, 27:413–419.

[Choung and Fung, 1986] Choung, C. and Fung, Y. (1986). Residual stress in arteries. In *Frontiers in Biomechanics*, pages 117–179. Springer-Verlag, New York.

[Duszyk et al., 1989] Duszyk, M., Schwab, B., Zahalak, G., Qian, H., and Elson, E. (1989). Cell poking: Quantitative analysis of indentation of thick viscoelastic layers. *Biophys J*, 55:683–690.

[Edwards et al., 1970] Edwards, R., Laferty, J., and Lange, K. (1970). Ligament strain in the human knee joint. *ASME J Basic Engng*, 92:131–136.

[Fung, 1981] Fung, Y. (1981). *Biomechanics: Mechanical Properties of Living Tissues.* Springer-Verlag, New York.

[Grood and Suntay, 1983] Grood, E. and Suntay, W. (1983). A joint coordinate system for the clinical description of three-dimensional motions: Application to the knee. *ASME J Biomech Engng*, 105:136–144.

[Guccione et al., 1991] Guccione, J., McCulloch, A., and Waldman, L. (1991). Passive material properties of intact ventricular myocarcium determine from a cylindrical model. *ASME J Biomech Engng*, 113:42–55.

[Hallquist et al., 1985] Hallquist, J., Goudreau, G., and Benson, D. (1985). Sliding interfaces with contact-impact in large scale Lagrangian computations. *Comp Meth Appl Mech Engng*, 51:107–137.

[Horowitz et al., 1988] Horowitz, A., Sheinman, I., and Lanir, Y. (1988). Nonlinear incompressible finite element for simulating loading of cardiac tissue - part ii: Three dimensional formulation for thick ventricular wall segments. *ASME J Biomech Engng*, 110:62–68.

[Humphrey et al., 1990] Humphrey, J., Strumph, R., and Yin, F. (1990). Determination of a constitutive relation for passive myocardium: I. A new functional form. *ASME J Biomech Engrg*, 112:333–339.

[Humphrey and Yin, 1987] Humphrey, J. and Yin, F. (1987). On constitutive relations and finite deformations of passive cardiac tissue: I. a pseudostrain-energy approach. *ASME J Biomech Engng*, 109:298–304.

[Johnson et al., 1994] Johnson, G., Tramaglini, D., Levine, R., Ohno, K., Choi, N., and Woo, S.-Y. (1994). Tensile and viscoelastic properties of human patellar tendon. *J Orthop Res*, 12:796–803.

[Lanir, 1980] Lanir, Y. (1980). A microstrucure model for the rheology of mammalian tendon. *ASME J Biomech Engng*, 102:332–339.

[Lanir, 1983] Lanir, Y. (1983). Constitutive equations for fibrous connective tissues. *J Biomechanics*, 16:1–12.

[Mak, 1986] Mak, A. (1986). The apparent viscoelastic behavior of articular cartilage - The contributions from the intrinsic matrix viscoelasticity and interstitial fluid flows. *ASME J Biomech Engng*, 108:123–130.

[Maker, 1994] Maker, B. (1994). Rigid bodies for metal forming analysis with NIKE3D. *Int J Num Methods Engng*, 37:1–18.

[Maker et al., 1990] Maker, B., Ferencz, R., and J.O., H. (1990). NIKE3D: A nonlinear, implicit, three-dimensional finite element code for solid and structural mechanics. *Lawrence Livermore National Laboratory Technical Report*, (UCRL-MA-105268).

[Marsden and Hughes, 1983] Marsden, J. and Hughes, T. (1983). *The Mathematical Foundations of Elascitity*. Prentice-Hall, Englewood Cliffs, New Jersey.

[Mills and Hull, 1991] Mills, O. and Hull, M. (1991). Flexibility of the human knee as a result of varus/valgus and axial moments in vivo: Experiments and results. *Skiing Trauma and Safety - 8th International Symposium*, STP-1104:35–56.

[Mooney, 1940] Mooney, M. (1940). A theory of large elastic deformation. *J Appl Phys*, 11:582–592.

[Neubert, 1963] Neubert, H. (1963). A simple model representing internal damping in solid materials. *The Aeronautical Quarterly*, 14:187–210.

[Pinto and Patitucci, 1980] Pinto, J. and Patitucci, P. (1980). Visco-elasticity of passive cardiac muscle. *ASME J Biomech Engng*, 102:57–61.

[Pradas and Calleja, 1990] Pradas, M. and Calleja, R. (1990). Nonlinear viscoelastic behavior of the flexor tendon of the human hand. *ASME J Biomech Engng*, 23:773–781.

[Setton et al., 1993] Setton, L., Zhu, W., and Mow, V. (1993). Biphasic poroviscoelastic behavior of articular cartilage: Role of the surface zone in governing the compressive behavior. *J Biomech*, 26:581–592.

[Simo and Taylor, 1991] Simo, J. and Taylor, R. (1991). Quasi-incompressible finite elasticity in principal stretches: Continuum basis and numerical algorithms. *Comp Meth Appl Mech Engng*, 85:273–310.

[Simo et al., 1985] Simo, J., Taylor, R., and Pister, K. (1985). Variational and projection methods for the volume constraint in finite deformation elastoplasticity. *Comp Meth Appl Mech Engng*, 51:177–208.

[Spencer, 1984] Spencer, A. (1984). *Continuum Theory of the Mechanics of Fibre-Reinforced Composites*. Springer-Verlag, New York.

[Suh et al., 1991] Suh, J.-K., Spilker, R., and Holmes, M. (1991). A penalty finite element formulation for soft hydrated tissues under finite deformation. *Int J Numer Methods Engng*, 32:1411–1439.

[Thielke et al., 1995] Thielke, R., Vanderby, R., and Grood, E. (1995). Volumetric changes in ligaments under tension. *Proc ASME Bioengineering Conference*, 29:197–198.

[Tschoegl, 1989] Tschoegl, N. (1989). *The Phenomenological Theory of Linear Viscoelastic Behavior*. Springer-Verlag, New York.

[Weiss, 1994] Weiss, J. (1994). *A constitutive model and finite element representation for transversely isotropic soft tissues*. Ph.D. Thesis, Department of Bioengineering, The University of Utah.

[Weiss, 1995] Weiss, J. (1995). A model for the material behavior of ligaments and tendons. *ASME Advances in Bioengineering*, BED-31:97–98.

[Weiss et al., 1995a] Weiss, J., Maker, B., and Govindjee, S. (1995a). Finite element implementation of incompressible, transversely isotropic hyperelasticity. *In Press, Computer Methods in Applied Mechanics and Engineering*, (UC Berkeley Report UCB/SEMM-95/07).

[Weiss et al., 1995b] Weiss, J., Maker, B., and Schauer, D. (1995b). Treatment of initial stress in hyperelastic finite element models of soft tissues. *ASME Bioengineering Conference*, BED-29:105–106.

[Woo et al., 1981] Woo, S.-Y., Gomez, M., and Akeson, W. (1981). The time- and history-dependent viscoelastic properties of the canine medial collateral ligament. *ASME J Biomech Engng*, 103:293–298.

[Woo et al., 1980] Woo, S.-Y., Simon, B., Kuei, S., and Akeson, W. (1980). Quasi-linear viscoelastic properties of normal articular cartilage. *ASME J Biomech Engng*, 102:85–90.

List of Tables

List of Figures

Table 1: Material Coefficients for A) Transversely Isotropic Elastic Response [Weiss, 1994, Weiss et al., 1995], B) Continuous Relaxation Function [Woo et al., 1981], and C) Discrete Series Approximation.

A)

C_1 (MPa)	C_2 (MPa)	C_3 (MPa)	C_4	C_5 (MPa)	λ^*
47.93	-40.46	2.36	76.90	1584.0	1.03

B)

τ_1 (seconds)	τ_2 (seconds)	C (seconds)
0.099	0.29	1.99 x 10^5

C)

G_e (MPa)	G_0 (MPa)	N_d	I_0
0.429	1.0	6	0

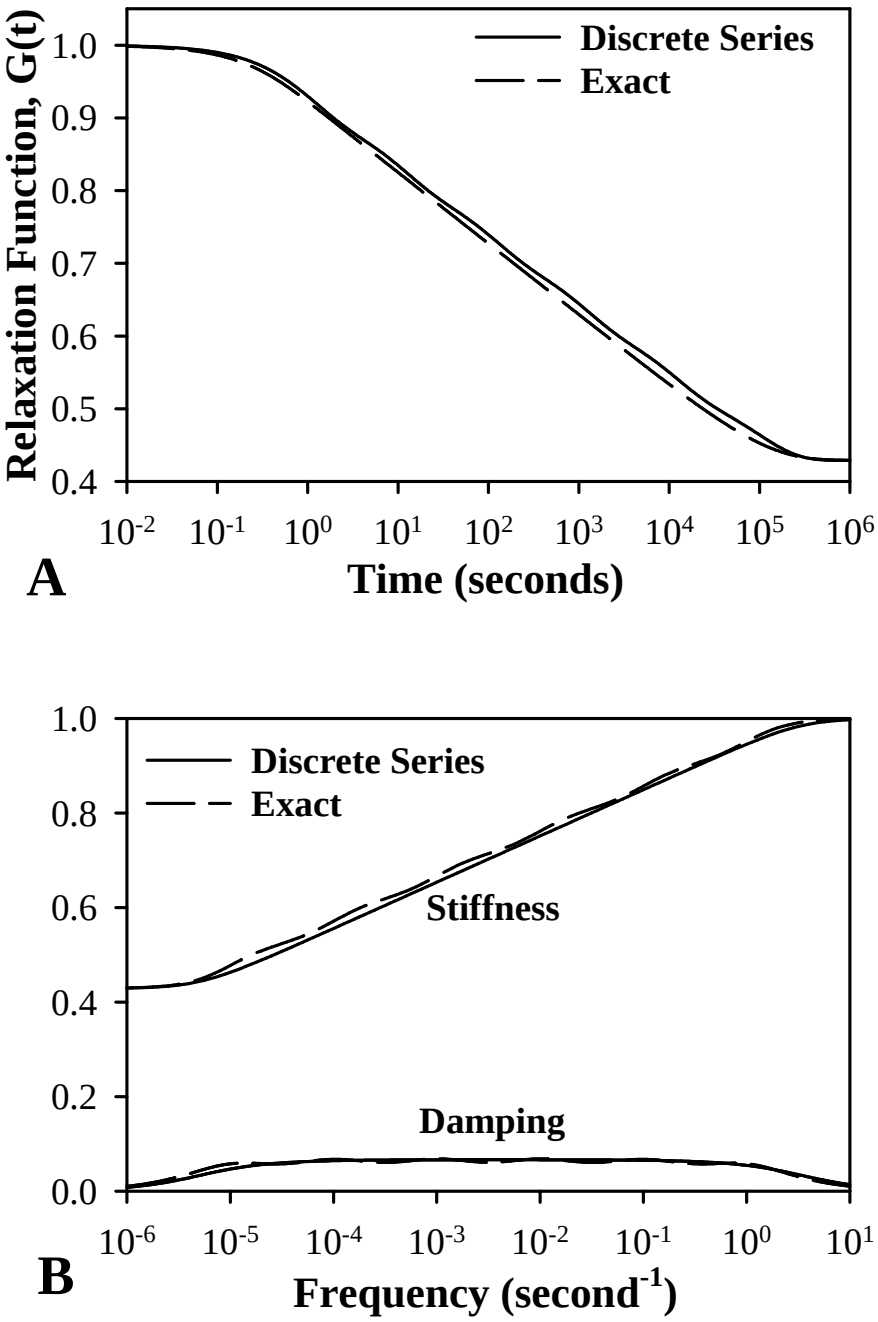

Figure 1: A) Reduced relaxation function $G(t)$ given by the quasilinear viscoelastic function (4) and the discrete spectrum approximation (13). Note that the function is normalized to the time-zero value and thus is unitless. B) Real part (stiffness) and imaginary part (damping) of the complex modulus given by the quasilinear viscoelastic function in (4), and the discrete spectrum approximation in (13). Note that the stiffness and damping are unitless - see equations (6) and (7). Coefficients for $G(t)$ are listed in Table 1A.

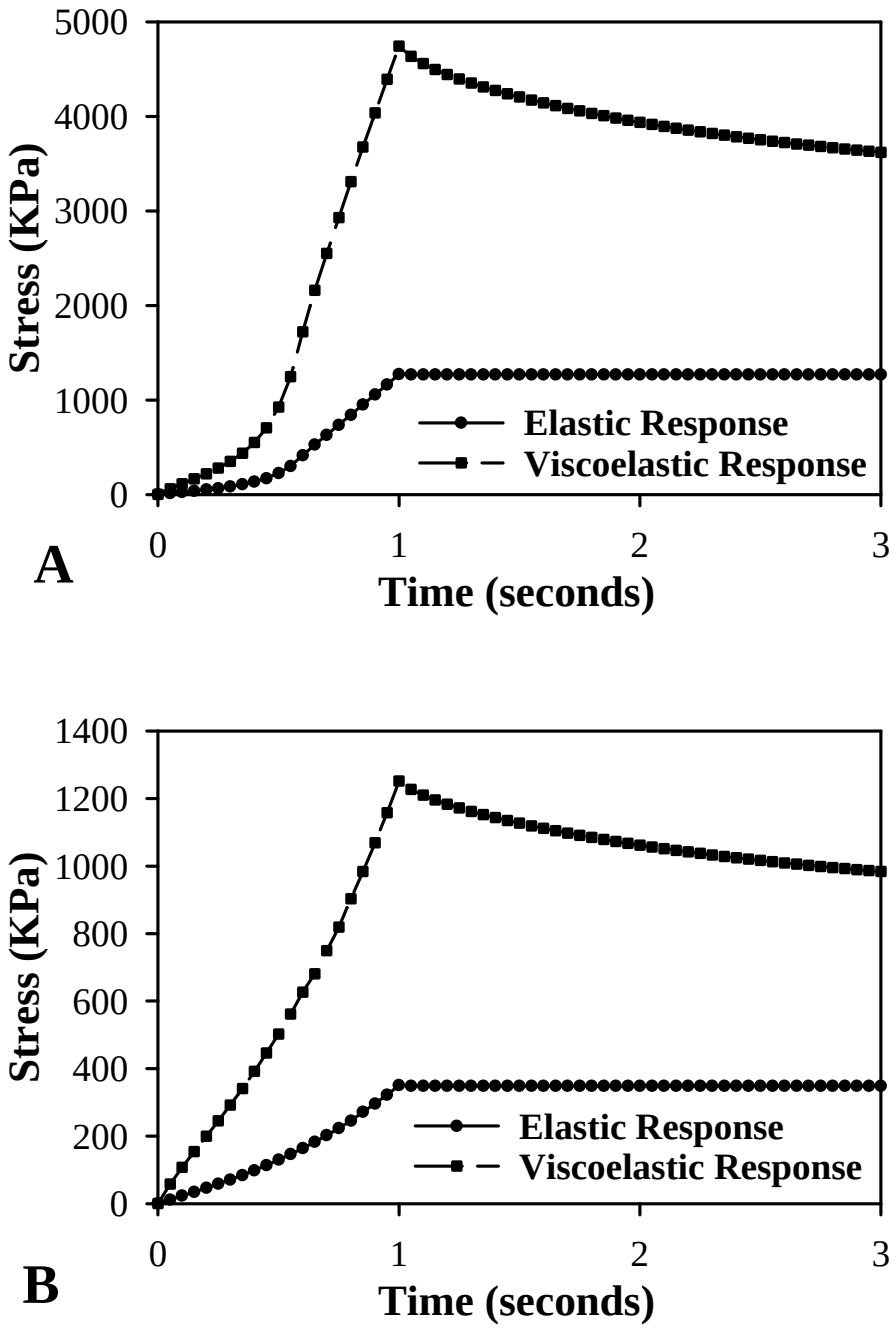

Figure 2: One-element simulation of equibiaxial stretch to 100% elongation followed by equibiaxial stress relaxation. Curves illustrate both the elastic and viscoelastic material cases. Data points represent computational times from the finite element code. A) stresses along the collagen fiber direction. B) stresses transverse to the collagen fiber direction.

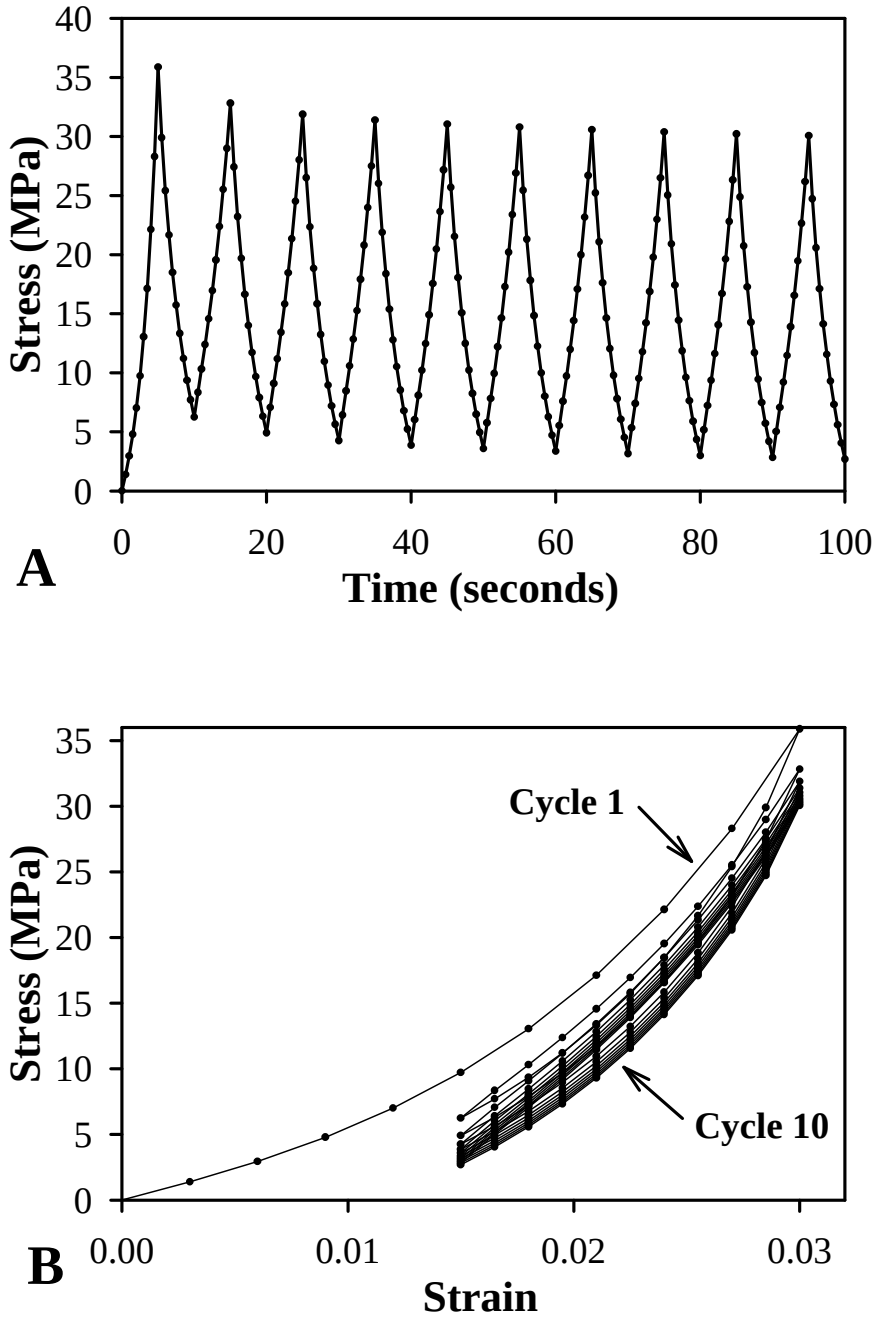

Figure 3: Finite element modeling of stress relaxation using the discrete spectrum approximation. Data points represent timestep intervals taken by the finite element code. A) Computed stress response versus time. Changes in the hysteresis curve with increasing cycle number are evident. B) Computed stress response versus applied strain. Note the decreases in peak and valley stresses with increasing cycle number.

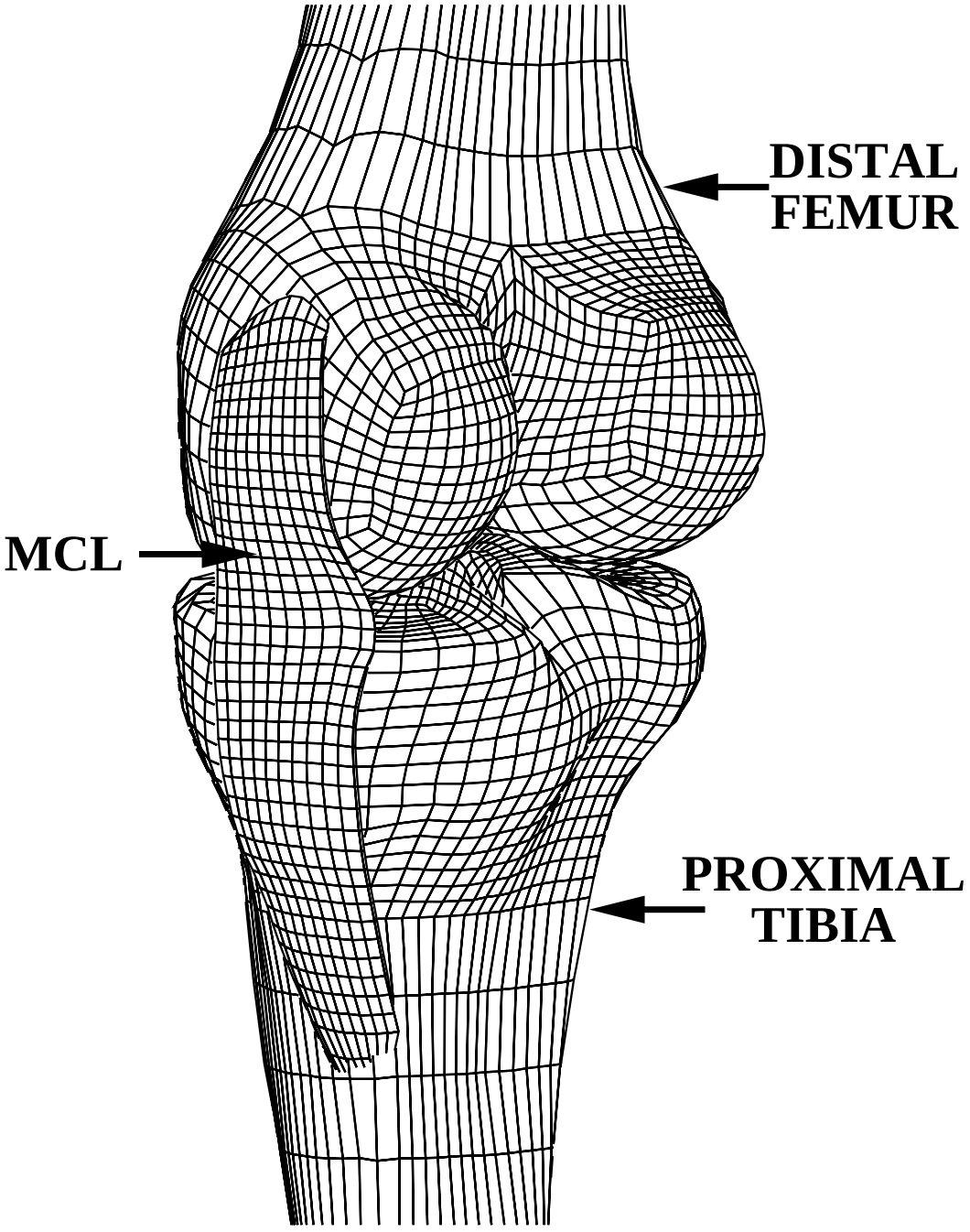

Figure 4: Detail of a finite element model of the human femur-MCL-tibia complex. The mesh was used with the visco-hyperelastic constitutive model to examine the stresses in the MCL during knee flexion.

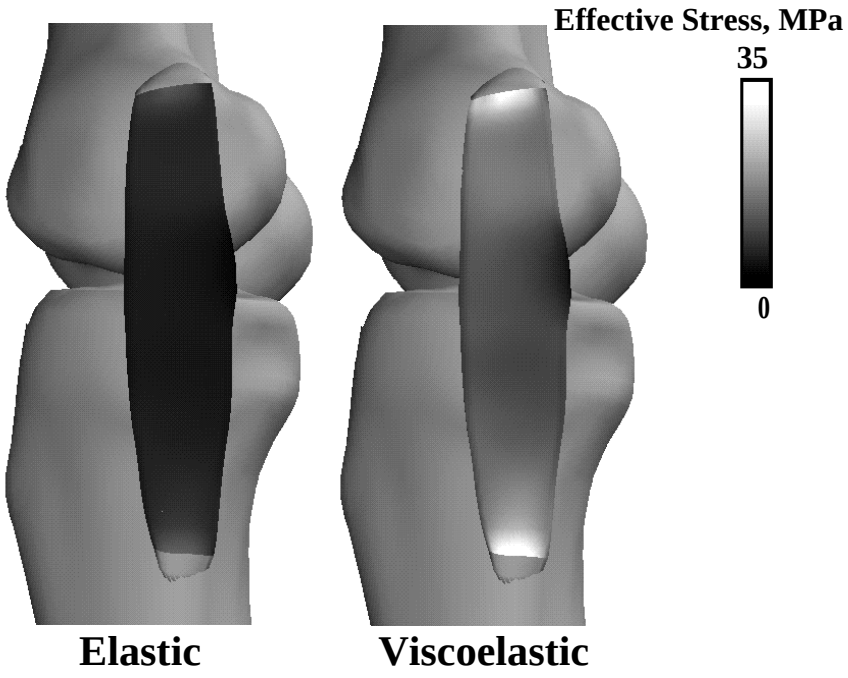

Figure 5: Effective (von Mises) stress in the MCL at 5 degress valgus rotation using both the hyperelastic (left) and visco-hyperelastic material models. The viscoelastic response resulted in higher peak stresses as a result of the rate effects on the material effective stiffness.